International Journal of Engineering Trends and Technology
ISSN: 2231 – 5381 /doi:10.14445/22315381/IJETT-V69I5P228
Volume 69 Issue 5, 208-227, May 2021

Modeling and Optimization of Process Parameters of Friction Stir Welding of Al-Li Alloy AA2050 by Response Surface Methodology

Raju Kamminana[#1], Venkatasubbaiah Kambagowni[*2]

[#] *Research Scholar, Department of Mechanical Engineering, Andhra University, Visakhapatnam, Andhra Pradesh, India. https://orcid.org/0000-0002-2947-7561*

[*]*Senior Professor and Head of the Department, Mechanical Engineering, Andhra University, Visakhapatnam, Andhra Pradesh, India. https://orcid.org/0000-0003-4440-2071*

[1]dkamminana@gmail.com, [2]drkvsau@yahoo.co.in

Abstract *- The third generation heat treatable Al-Li alloy AA2050 has extensive applications in automotive, defense, and air-craft industries due to its excellent corrosion resistance and high strength-to-weight ratio. Friction stir welding (FSW) is a novel solid-state joining technique suitable for aluminum alloys compared to conventional fusion welding techniques. This investigation presents the development of mathematical models with four numerical process parameters (traverse speed, rotational speed, tilt angle, and shoulder diameter) and one categorical process parameter (tool pin profile) to predict the responses of the friction stir weld joint of AA2050-T84, viz tensile strength, yield strength, elongation, hardness, bending load and width of the heat-affected zone. The optimal (combined) design was used to design the experiments with five factors and four levels. Analysis of variance was used to validate the developed mathematical models, and the desirability approach in response surface methodology (RSM) was used to find the optimum parameters of the multi-response problem.*

Keywords — *Friction stir welding, analysis of variance, desirability approach, multi-response optimization, response surface methodology*

I. INTRODUCTION

Friction stir welding (FSW) is a relatively novel welding technique compared to conventional fusion welding techniques. In the year 1991, The Welding Institute Ltd. invented this solid-state joining technique, and it has been developed rapidly over the years. FSW is a more suitable joining method for heat treatable aluminum alloys. The fusion welding of the heat treatable aluminum alloys leads to various defects such as shrinkage, embrittlement, residual stresses, hot cracking, and distortion [1, 2]. Infusion welding, melting above the eutectic point and solidification leads to the brittle interdendritic formation, results in a decrease in mechanical properties [3]. The FSW is free from fusion welding defects, and also refinement of microstructure occurs due to dynamic recrystallization [4].

FSW of heat treatable aluminum alloys finds applications in automotive, aircraft, and defense equipment fabrication. FSW is a popular joining method of aluminum alloys of 2000, 5000, 6000, 7000, aluminum-lithium series, and aluminum composites [5]. In this work, the FSW of third-generation Al-Li alloy AA2050 has been taken up. The alloy is heat-treated in solution, artificially underaged, and cold worked (T84). The base metal has an ultimate tensile strength of 585 MPa, yield strength of 565 MPa, and tensile elongation of 8% [6].

G.Elatharasan *et al.* [7] carried FSW of dissimilar aluminum alloys AA6061-T6 and AA7075-T6 and used RSM to develop quadratic models for the response variables, namely ultimate tensile strength, yield strength, and displacement in terms of process parameters (traverse speed, rotational speed, and axial force). Analysis of variance (ANOVA) was used to test the adequacy of the developed models and desirability approach was used to optimize the responses. A.Heidarzadeh *et al.* [8] investigated the optimization of process parameters (welding speed, rotational tool speed, and axial force) of FSW of aluminum alloy AA6061-T4. The experiments were designed based on central composite rotatable design and mathematical models

Table 1. Composition of AA2050 by the percentage of weight

Si	Fe	Cu	Mg	Mn	Li	Ti	Zn	Zr	Ag	Al
0.0354	0.0511	3.53	0.358	0.345	0.85	0.0375	0.0328	0.0868	0.363	94.2

Were developed to predict tensile strength and tensile elongation. The models were validated by ANOVA, and optimum process parameters were evaluated by the RSM. R.Palanivel *et al.* [9] presented the use of response surface methodology (RSM) to optimize the process parameters (welding speed, rotational tool speed, and axial force) of FSW of aluminum alloy AA5083-H111. Three factors five-level central composite rotatable design was used to design the experiments. The adequacy of the linear model developed by RSM was checked by ANOVA. The process parameters were optimized using RSM to maximize the ultimate tensile strength. G.Elatharasan *et al.* [10] designed the experiment with three input parameters of FSW of aluminum alloy AA6061 – T6 (welding speed, rotational speed, and axial force), with three levels and 20 runs using the Central Composite Design (CCD). They developed the mathematical relationship between input parameters and the responses (tensile strength, yield strength, and ductility). They also evaluated the effect of input parameters on responses and validated the models using ANOVA. They found the optimum values of parameters using the desirability approach. Divya Deep Dhancholia *et al.* [11] optimized the process parameters of FSW of dissimilar aluminum alloys AA6061 and AA7039. The experiments were designed according to the central composite design (CCD) with two factors (traverse speed and rotational speed) at two levels. Tensile strength, yield strength, impact strength, and hardness were considered as responses, and the parametric optimization was carried by RSM. R.Kadaganchi *et al.* [12] studied the optimization of parameters in the FSW of aluminum alloy AA2014-T6. Tool traverse speed, rotational speed, tilt angle, and too pin profile were selected for study the effect of parameters on the responses (Ultimate tensile strength, Yield Strength and % elongation). The experiments were designed using the central composite design (CCD), and mathematical models to predict responses were developed. The adequacy of the developed models was assessed by the ANOVA and determined optimum process parameter values to get the maximum responses using RSM. A.Farzadi *et al.* [13] employed RSM to optimize the process parameters (welding speed, rotational speed, pin diameter, and shoulder diameter) of FSW of aluminum alloy AA7075-T6. Five levels of four factors were taken to design experiments with central composite design (CCD). ANOVA showed that rotational speed and welding speed have a greater impact on the response, i.e., tensile strength. B.Ravi Sankar *et al.* [14] aimed to optimize the process parameters (welding speed, rotational speed, and pin diameter) of the FSW joint of aluminum alloy AA6061. The experiments were designed with three factors five-level response surface design. The mathematical models were developed, and the optimum values of parameters to maximize the hardness and tensile strength were identified from the response surface plots. A.Goyal *et al.* [15] investigated the influence of process parameters (welding speed, rotational speed, shoulder diameter, tool hardness, tool pin profile, and tilt angle) on the inter-granular corrosion rate of FSW joint of aluminum alloy AA5086-H32. The experiments were designed according to the central composite design (CCD) and a mathematical model was developed for the response in terms of parameters. The adequacy of the model and the significance of the process parameters were evaluated by ANOVA. RSM was used to find the optimum set of parameters to minimize the corrosion rate.

It is observed from the above literature that RSM was successfully implemented to either single-response or multi-response optimization problems. Hence, in this investigation, RSM is selected to optimize the problem of multi-response FSW of aluminum alloy AA2050-T84 on which little work has been carried. The significant process parameters taken for this study are traverse speed, rotational speed, tilt angle, shoulder diameter, and tool pin profile. To carry a more comprehensive work, seven responses are selected. Namely, tensile strength, yield strength, elongation, hardness of weld zone, hardness of heat-affected zone, bending load, and width of the heat-affected zone.

II. EXPERIMENTAL WORK

A. Identifying the Significant Process Parameters and their Range

The significant process parameters affecting the responses were selected from the literature survey. The process parameters identified were traverse speed, rotational speed, tilt angle, shoulder diameter, and tool pin profile. The range of the selected parameters was decided from the literature, and the successful trial experiments carried with different combinations of process parameters. The process parameters and their range for the different aluminum alloys in the previous works were furnished in Table 2.

The levels of the process parameters are furnished in Table 3, and the geometry of the tool pin profiles is shown in Figure 1.

B. Design of Experiments

In this study, we have four numerical factors (traverse speed, rotational speed, tilt angle, shoulder diameter) and a categorical factor. Response surface methodology (RSM) based optimal (combined) design was used to accommodate both the numerical factors and categorical factors. Sixteen

Table 2. Previous works of FSW of Aluminium alloys with parameters and their range

Author & Year of Publication	The material selected for study	Parameters Selected	Range of process parameters
Mustafa Boz *et al*., (2004) [16]	AA1080	Tool Pin Profile	Square and cylindrical pins
P.Caraliere *et al.*, (2006) [17]	AA6056	Rotational speed and Traverse speed	Rotational speeds: 500-1000 rpm, traverse speeds:40-80 mm/min
K.Elangovan *et al*., (2007) [18]	AA2219	Rotational speed and tool pin profile	Rotational speeds: 800-1600 rpm and tool pin profiles: straight cylindrical, taper cylindrical, straight square, triangular and threaded cylindrical
K.Elangovan *et al*., (2008) [19]	AA2219	Traverse speed and tool pin profile	Traverse speeds: 22-75 mm/min, tool pin profiles: straight cylindrical, taper cylindrical, straight square, triangular and threaded cylindrical
Hannalie Lombard *et al.*, (2009) [20]	AA5083	Rotational speed and traverse speed	Rotational speeds: 254-870 rpm, traverse speeds: 85-185 mm/min
Kanwer S Arora *et al.*, (2010) [21]	AA2219	Shoulder diameter, rotational speed, tool pin diameter, and traverse speed	Shoulder diameters: 18-22 mm, rotational speeds: 250-400 rpm, traverse speeds: 60-180 mm/min, pin diameters: 7-9 mm
Loganathan Karthikeyan *et al*., (2011) [22]	AA6063	Traverse speed, rotational speed, and axial force	Traverse speeds: 22.2-75 mm/min, rotational speeds 800-1600 rpm, axial forces: 8-12 kN
Z. Barlas *et al.*, (2012) [23]	AA5754	Rotational speed, tool tilt angle, and tool rotation direction	Rotational speeds: 700-1100 rpm, tilt angles: 0-2 degrees, tool rotation directions: clockwise, counterclockwise
Muhsin *et al.*, (2012) [24]	AA7020	Traverse speed and rotational speed	Rotational speeds: 710-1400 rpm, traverse speeds: 16-40 mm/min
K.Ramanjeneyulu *et al.*, (2013) [25]	AA2014	Tool pin profile	Conical, triangular, square, pentagon, and hexagon
Suyash Tiwari *et al*., (2014) [26]	AA6063	Shoulder diameter, tool pin length, rotational speed, and traverse speed	Shoulder diameters: 16-20 mm, pin lengths: 1-2.8 mm, rotational speeds: 800-1600 rpm, traverse speed 60-100 mm/min
Ravindra S.Thube *et al.*, (2014) [27]	AA5083	Rotational speed and tool profile	Rotational speeds: 900-1800 rpm, tool pin profiles: cylindrical, taper cylindrical, square, triangular, cone
Emad Salari *et al*., (2014) [28]	AA5456	Rotational speed and tool geometry	Rotational speeds: 600-800 rpm, tool pin profiles: conical thread pin, cylindrical-conical thread pin, stepped conical thread pin, flared triflute pin
Joon-Tae Yoo *et al*., (2015) [29]	AA2195	Traverse speed and rotational speed	Traverse speeds: 120-360 mm/min, rotational speeds: 300-800rpm
A.Farzadi *et al.*, (2017) [13]	AA7075	Traverse speed, rotational speed, shoulder diameter, and pin diameter	Traverse speeds:35-95 mm/min, rotational speeds: 350-650 rpm, shoulder diameters: 12-18 mm, pin diameters: 4-6 mm
B.Ravi Sankar *et al*., (2017) [14]	AA6061	Traverse speed, rotational speed, and pin diameter	Traverse speeds: 30-55 mm/min, rotational speeds: 800-1400 rpm, pin diameters: 4-8 mm
V.K.Parikh *et al.*, (2017) [30]	AA2014	Traverse speed, rotational speed, and shoulder diameter	Traverse speeds: 80-125 mm/min, rotational speeds: 710-1400, shoulder diameters: 15-19 mm

Subham Verma *et al.*, (2018) [31]	AA6082	Traverse speed and rotational speed	Traverse speeds:20-100 mm/min, rotational speeds: 500-2000 rpm
Shanavas Shamsudeen *et al.*, (2018) [32]	AA5052	Traverse speed, rotational speed, tilt angle, and tool pin profile	Traverse speeds: 45-85 mm/min, rotational speeds: 400-800 rpm, tilt angle: 0.5-2.5 degrees, tool pin profiles: hexagon, pentagon, square, cylindrical, triangular
Abuajila *et al.*, (2018) [33]	AA5083	Traverse speed, rotational speed, and tilt angle	Traverse speeds: 75-150 mm/min, rotational speeds: 500-800 rpm, tilt angle 1-4 degrees
M.Gomathisankar *et al.*, (2018) [34]	AA6061	Traverse speed, rotational speed, dwell time, and tilt angle	Traverse speeds: 20-63 mm/min, rotational speeds: 450-710 rpm, dwell times 1.5 -2.5 min, tilt angles: 0-2 degrees
P.Pradeep Kumar *et al.*, (2019) [35]	AA7075	Traverse speed and rotational speed	Traverse speeds: 20-40 mm/min, rotational speeds: 1000-1400 rpm
A.Goyal *et al.*, (2019) [15]	AA5086	Traverse speed, rotational speed, shoulder diameter, tool hardness, tool pin profile and tilt angle	Traverse speeds: 37-132 mm/min, rotational speeds: 724-1675 rpm, shoulder diameters: 7.8 -22.1 mm, tool harnesses: 33-56 HRC, tilt angles: 0.8-3.2 degrees, tool pin profiles: straight cylindrical, pentagonal, hexagonal, square, threaded cylindrical

Table 3. Process parameters and their levels

S.NO	PROCESS PARAMETER	SYMBOL	UNIT	RANGE			
				LEVEL1	LEVEL 2	LEVEL 3	LEVEL 4
1	Traverse Speed	TS	mm/min	80	100	125	160
2	Rotational Speed	RS	rpm	900	1120	1400	1800
3	Tilt Angle	TA	degrees	0.5	1	1.5	2
4	Shoulder Diameter	SD	mm	16	18	20	22
5	Tool Pin Profile	TPP	_	SCL	TCL	SSQ	TSQ

SCL-Straight Cylindrical, TCL-Taper Cylindrical, SSQ-Straight Square, TSQ-Taper Square

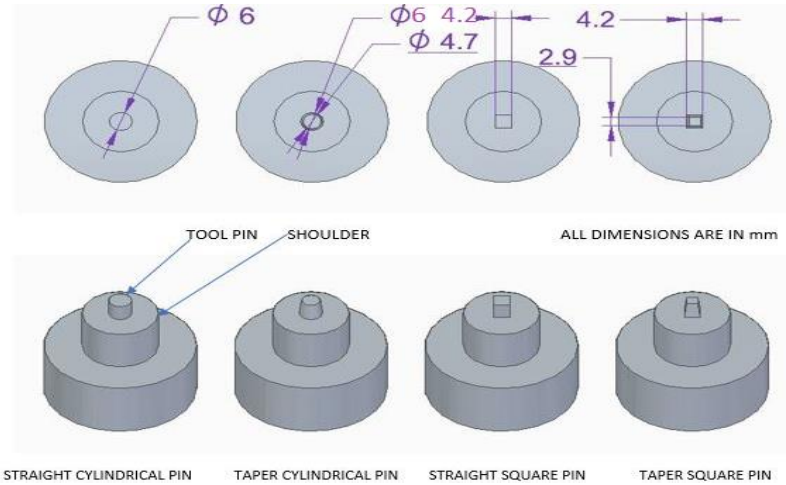

Fig. 1 Geometry of tool pin profiles

factorial points for the four numerical factors (2^4), five replicates at the central points and five lack-of-fit points were part of this design of experiment. Hence, the required number of experimental runs was 26 and the design with substituted factor levels was shown in the Table 4.

C. Experimental setup and testing of weld specimens

Friction stir welding (FSW) was carried on FN2EV model knee type milling machine made by HMT Ltd., Pinjore, India. The work pieces of 200 X 150 X 4 mm were securely clamped by the special fixtures. The square butt welding was carried along the length in a single pass. The tools of specified shoulder diameter and pin profile were made of AISI H13 tool steel. The sixteen tools were made with a probe length of 3.8 mm.

Tensile tests were conducted according to the standards IS1608 (Part-1):2018 on universal testing machine FIE-UTES40. Hardness tests (HV5) were carried according to the standards IS1501 (Part-1):2020 on Vickers hardness testing machine with a load of 5kgf. Bending tests was conducted according to the standards IS1599:2019 on universal testing machine FIE-UTES40 by fixing a bending jig with of 25 mm diameter mandrel. Inverted metallurgical microscope DEWINTER-1500X was used to measure the width of the heat affected zone. The test results along with the experimental design are furnished in the Table 4. The macrographs of the resulted weld beads are presented in the Figure 2.

Table. 4 Experimental design and their results

RUN	TS	RS	TA	SD	TPP	Tensile Strength (MPa)	Yield Strength (MPa)	% Elongation	Hardness of Weld Zone	Hardness of HAZ	Bending Load (N)	Width of HAZ µm
1	100	1400	2	22	TCL	259.39	228.28	2.20	105.5	114	3260	1974.133
2	160	1120	2	18	SSQ	336.35	240.74	4.30	102	119	1200	1645.269
3	100	1800	0.5	16	SSQ	224.80	209.14	2.56	105.5	111	1360	1074.459
4	160	1800	0.5	20	TCL	181.94	160.98	1.84	105.75	105	1460	1348.519
5	125	1800	1	22	TSQ	221.25	201.37	2.06	105.75	111.25	1860	1591.777
6	125	1120	1.5	20	TCL	296.10	240.27	2.28	106.5	111.9	2180	1504.893
7	100	1800	1.5	18	SCL	244.20	211.46	2.26	107.5	109.75	1280	1624.789
8	125	1400	0.5	18	SSQ	273.53	255.49	3.36	96.5	120	1240	1004.7
9	125	1120	1.5	20	TCL	281.61	236.71	2.34	107	110.75	1860	1582.537
10	100	900	2	20	TSQ	335.63	255.51	2.26	101	112.25	2980	1744.238
11	80	900	0.5	22	SCL	291.70	238.31	3.20	103	112.25	1520	1994.353
12	125	1800	1	22	TSQ	230.03	210.16	1.98	107	111	1520	1656.54
13	80	1800	1	20	SSQ	228.74	200.70	2.86	105	116	960	1648.51
14	160	1120	2	22	SCL	326.73	232.61	3.96	108.5	111	1460	1763.343
15	100	1400	1	20	SCL	280.08	226.78	2.96	103	103	1080	1598.176
16	125	900	2	16	SCL	355.71	252.03	2.10	103.75	107.75	1610	1338.095
17	80	1400	1.5	20	TSQ	226.67	213.33	1.86	105	108.5	2620	1984.864
18	160	1400	1.5	16	TSQ	240.54	227.41	1.52	107.5	117.25	2460	1252.413
19	100	1120	0.5	18	TSQ	291.62	271.34	2.06	108	115.25	3180	1279.056
20	80	1800	2	18	TCL	226.27	213.19	1.88	107	110.75	1260	1566.674
21	160	900	1	18	TCL	278.42	207.53	2.56	101.5	117.75	1780	1394.903
22	80	900	0.5	22	SCL	284.45	224.65	3.12	102.5	111.75	1380	2054.387
23	80	1120	1	16	TCL	250.75	238.91	2.72	106	112.25	1840	1262.41
24	100	900	1.5	22	SSQ	340.85	255.02	4.20	98.5	120.5	1280	1863.645
25	160	900	1	18	TCL	260.39	216.54	2.62	102.75	115.75	1940	1414.534
26	100	1800	1.5	18	SCL	239.35	219.95	2.32	107	105.25	1040	1604.986

III. METHODOLOGY

A. Response Surface Methodology

Response surface methodology (RSM) is a conventional optimization method, which combines regression analysis with statistical techniques to design the experiments, develop a mathematical model and find the process parameter values in order to maximize or minimize the response properties. The mathematical model developed can predict the dependent variable (response) in terms of independent variables (parameters). The regression model developed can also geometrically represent the surface, when plotted for response versus any two parameters. We can visualize the relation between response and selected parameters from the 3-D response surface plots. Corresponding contour plots of response surface helps us to locate the parameter values that yields optimum response value. The regression model is in the form of

$$X = \beta_o + \sum_{i=1}^{n} \beta_i Y_i + \sum_{i=1}^{n} \beta_{ii} Y_i^2 + \sum_{i=1}^{n} \sum_{j=i+1}^{n} \beta_{ij} Y_i Y_j + \varphi \quad (1)$$

Where X = response; φ random error; n the number of independent variables; β_o coefficient of constant; β_i coefficients of linear terms; β_{ii} coefficients of quadratic terms; β_{ij} coefficients of interaction terms; Y_i and Y_j coded values of the process parameters.

B. Testing for adequacy of model

The acceptability of the developed model can be decided from regression analysis and the analysis of variance (ANOVA). The regression analysis gives the values of coefficient of determination (R^2), adjusted R^2 and predicted R^2, which are need to be in reasonable agreement. The higher the value of R^2 (nearer to 1), better the model explains the variability in the data. In the ANOVA the adequacy of the model is checked by 'F-test' and 'p-value'. If the F-value calculated is less than the F-value in the table for the given confidence level, then the model is adequate to explain the variance in the data. Similarly if the p-value of model is less than 0.05, the model is significant. The ANOVA and the fit statistics were carried by the Design Expert 12 software.

C. Optimization of process parameters –Desirability Approach

To solve the multi-response problem with response surface methodology (RSM), desirability approach is used. It is flexible, simple and available in RSM software. This method combines all the responses into a dimensionless 'measure of performance' known as the combined desirability function, which varies between 0 and 1. The design expert 12 software was used to carry the desirability approach.

IV. RESULTS AND DISCUSSION

A. Effect of Process Parameters on Tensile Strength

Response surface plots such as 3-D surface plots and 2-D contour plots are used to establish the desirable response values and corresponding process parameters. The surface plots and contour plots are drawn for each response versus any of the two significant process parameters. The remaining process parameters are fixed at a given point, usually at the mean value. The surface plot displays a 3-D view that provides clear details of variation of response. The contour plot is rectangular representation of surface plot, shows the contour lines, which are constant response lines.

To study the effect of process parameters on the individual response, two relatively more significant interaction terms were selected for each response. For tensile strength, interaction effects of traverse speed-shoulder diameter (AD) and rotational speed-shoulder diameter (BD) were identified as significant terms based on the ANOVA results shown in the Table 5. The maximum predicted value for tensile strength of 337.363 MPa at desirability of 0.89442 was obtained at transverse speed of 90 mm/min, rotational speed of 900 rpm and shoulder diameter of 16 mm. At a shoulder diameter of 16 mm, the tensile strength was initially increasing with the traverse speed up to 90 mm/min and then decreasing. At a traverse speed of 90 mm/min, the tensile strength was slightly decreasing with respect to shoulder diameter. At a shoulder diameter of 16 mm, the tensile strength was decreasing with respect to rotational speed. At a rotational speed of 900 rpm, the tensile strength was slightly decreasing with respect to shoulder diameter. The colour coding in the contour plots in the Figure 2 and Figure 3 suggest that better values for tensile strength will be resulted at the lower values than the lower limits of rotational speed and shoulder diameter taken in this work.

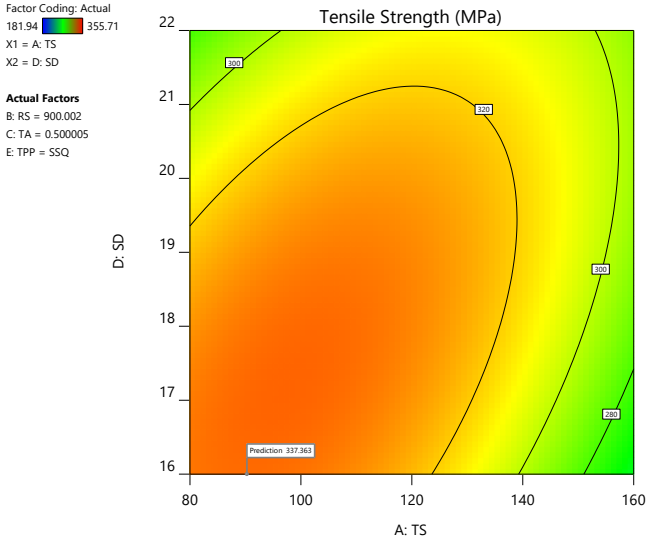

Fig. 2 Effects of TS and SD on tensile strength

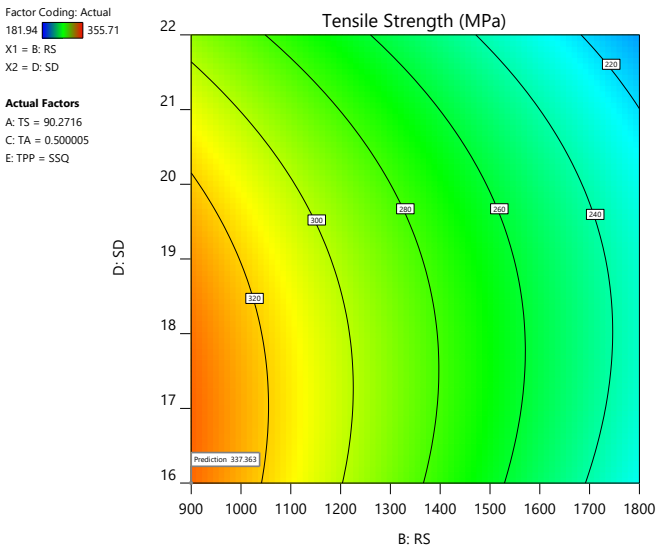

Fig. 3 Effects of RS and SD on tensile strength

a) Models Developed for Tensile Strength: The mathematical models for tensile strength in terms of process parameters were developed by the RSM for the four tool pin profiles. The regression models, which are reduced quadratic models, can predict the tensile strength for the process parameters values within the selected range. The substitution of process parameters in the regression model should be with their original units. The models for tensile strength for different tool pin profiles are shown in the Eq. (2) – Eq. (5).

TPP: **SCL**

Tensile Strength = +176.99771 +0.458108*TS - 0.198769*RS 69.47516*TA +34.89356*SD +0.178385*TS*SD +0.004737*RS*SD -0.015454*TS² +29.37287*TA² -1.64413*SD² (2)

TPP: **TCL**

Tensile Strength = +93.11704+0.442497*TS -0.198769*RS - 35.57430*TA +34.89356*SD +0.178385*TS*SD +0.004737*RS*SD -0.015454*TS² +29.37287*TA² - 1.64413*SD² (3)

TPP: **SSQ**

Tensile Strength = +189.04178 -0.069090*TS -0.198769*RS -22.42650*TA +34.89356*SD +0.178385*TS*SD +0.004737*RS*SD -0.015454*TS² +29.37287*TA² - 1.64413*SD² (4)

TPP: **TSQ**

Tensile Strength = +90.32395 +0.866544*TS -0.198769*RS -53.64991*TA +34.89356*SD +0.178385*TS*SD +0.004737*RS*SD -0.015454*TS² +29.37287*TA² - 1.64413*SD² (5)

b) Adequacy of the Models: The mathematical models developed in the section 4.1.1 were validated by the analysis of variance (ANOVA) and the results are shown in the Table 5. The adequacy of the model and significance of process parameters were evaluated by the ANOVA. The adequacy of model was decided from the F-value and fit statistics. The significance was decided from the p-value. The model and process parameters, whose p-value was less than 0.05 were significant. The models developed for tensile strength were adequate and significant as its F-value is large (51.99) and p-value is very small (<0.0001). The lack of fit of the models were not significant as its F-value is very small (0.1297) and p-value is greater than 0.05 (0.8813). The terms B (RS), C (TA), E (TPP), A^2, C^2 and D^2 were significant terms in the model as their respective p-values are less than 0.05.

The fit statistics of the models developed for the tensile strength are shown in the Table 6. The high value of coefficient of determination R^2 (0.9926) indicates the adequacy and fitness (ability to explain the variation in the data) of the model. The difference between adjusted R^2 (0.9735) and predicted R^2 (0.7763) is less than 0.2, which is a good indicator of fitness of the model. The strength of signal compared to noise is decided by the adequate precision ratio. A minimum value of 4 for the adequate precision indicates the adequate signal, which is 28.1737 in this case. The small value of standard deviation (7.19) compared to the mean (269.5) indicates the accuracy of the model to predict the tensile strength compared to the actual value.

Table 5. ANOVA for tensile strength model

Source	Sum of Squares	df	Mean Square	F-value	p-value		% Contribution
Model	48385.97	18	2688.11	51.99	< 0.0001	significant	
A-TS	12.08	1	12.08	0.2336	0.6436		0.08
B-RS	6973.37	1	6973.37	134.86	< 0.0001	significant	45.24
C-TA	1148.33	1	1148.33	22.21	0.0022	significant	7.45
D-SD	192.19	1	192.19	3.72	0.0952		1.25
E-TPP	6047.26	3	2015.75	38.98	< 0.0001	significant	13.08
AD	212.27	1	212.27	4.11	0.0824		1.38
AE	607.19	3	202.4	3.91	0.0624		1.31

BD	119.85	1	119.85	2.32	0.1717		0.78
CE	466.03	3	155.34	3	0.1043		1.01
A^2	522.57	1	522.57	10.11	0.0155	significant	3.39
C^2	770.03	1	770.03	14.89	0.0062	significant	4.99
D^2	395.97	1	395.97	7.66	0.0278	significant	2.57
Residual	361.95	7	51.71				
Lack of Fit	17.85	2	8.92	0.1297	0.8813	not significant	
Pure Error	344.11	5	68.82				
Cor Total	48747.92	25					

Table 6. Fit statistics for tensile strength model

Standard deviation	7.19	**R^2**	0.9926
Mean	269.50	**Adjusted R^2**	0.9735
C.V. %	2.67	**Predicted R^2**	0.7763
		Adequate Precision	28.1737

B. Effect of Process Parameters on Yield Strength

For yield strength interaction effects of traverse speed-shoulder diameter (AD) and rotational speed-tilt angle (BC) were identified as significant terms based on the ANOVA results shown in the Table 7. The maximum predicted value for yield strength of 324.497 MPa at desirability of 1 was obtained at traverse speed of 90 mm/min, rotational speed of 900 rpm and shoulder diameter of 16 mm. At a shoulder diameter of 16 mm, the yield strength was initially increasing with the traverse speed up to 90 mm/min and then decreasing. At a traverse speed of 90 mm/min, the yield strength was gradually decreasing with respect to the shoulder diameter. At a rotational speed of 900 rpm the yield strength was constant with respect to the tilt angle. At a tilt angle of 0.5^0, yield strength was drastically decreasing with respect to the rotational speed. The colour coding in the contour plots in the Figure 4 and Figure 5 suggest that range of process parameters selected were good enough to get high value of yield strength.

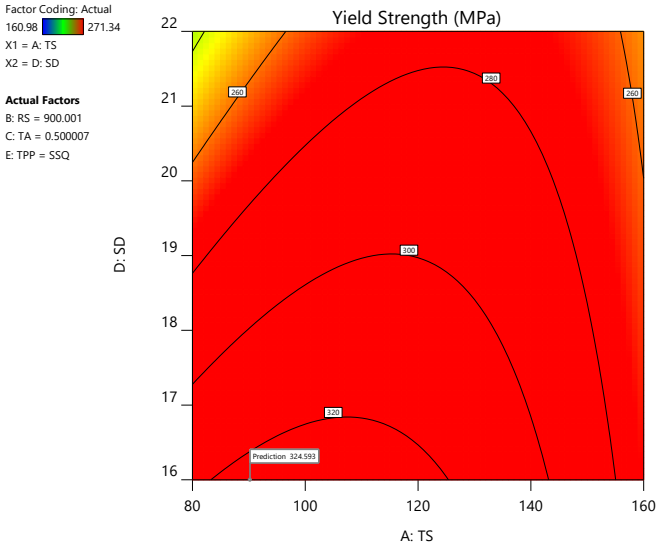

Fig. 4 Effects of TS and SD on yield strength

a) Models Developed for Yield Strength: The mathematical models for yield strength in terms of process parameters were developed by the RSM for the four tool pin profiles. The regression models, which are reduced quadratic models, can predict the yield strength for the process parameters values within the selected range. The substitution of process parameters in the regression model should be with their original units. The models for yield strength for different tool pin profiles are shown in the Eq. (6) – Eq. (9).

TPP: **SCL**

Yield Strength= +647.74068 +1.47107*TS -0.349851*RS -42.10837*TA -25.26846*SD +0.000376*TS*RS -0.163227*TS*TA +0.137158*TS*SD +0.057690*RS*TA +0.009573*RS*SD -0.018798*TS^2 (6)

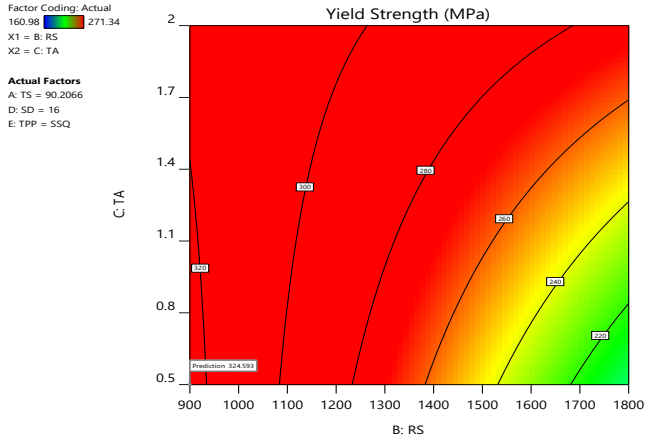

Fig. 5 Effects of RS and TA on yield strength

TPP: **TCL**

Yield Strength= +717.13418 +1.47107*TS -0.349851*RS - 42.10837*TA -29.55158*SD +0.000376*TS*RS - 0.163227*TS*TA +0.137158*TS*SD +0.057690*RS*TA +0.009573RS*SD -0.018798*TS² (7)

TPP: **SSQ**

Yield Strength= +824.79050 +1.47107*TS -0.349851*RS - 42.10837*TA -33.05920*SD +0.000376*TS*RS - 0.163227*TS*TA +0.137158*TS*SD +0.057690*RS*TA +0.009573*RS*SD -0.018798*TS² (8)

TPP: **TSQ**

Yield Strength= +913.49736 +1.47107*TS -0.349851*RS - 42.10837*TA -38.64181*SD +0.000376*TS*RS - 0.163227*TS*TA +0.137158*TS*SD +0.057690*RS*TA +0.009573*RS*SD -0.018798*TS² (9)

b) Adequacy of the Models: The mathematical models developed in the section 4.2.1 were validated by the analysis of variance (ANOVA) and the results are shown in the Table 7. The models developed for yield strength were adequate and significant as its F-value is large (27.45) and p-value is very small (<0.0001). The lack-of-fit of the models were not significant as its F-value is very small (0.2952) and p-value is greater than 0.05 (0.8697). All the process parameters along with the interactive terms AB, AD, BC, BD, DE and A^2 were significant terms in the model as their respective p-values are less than 0.05.

The fit statistics of the models developed for the yield strength are shown in the Table 8. The high value of coefficient of determination R^2 (0.9799) indicates the adequacy and fitness of the model. The difference between adjusted R^2 (0.9422) and predicted R^2 (0.8092) is less than 0.2, which is a good indicator of fitness of the model. A minimum value of 4 for the adequate precision indicates the adequate signal, which is 25.0802 in this case. The small value of standard deviation (5.43) compared to the mean (226.48) indicates the accuracy of the model to predict the yield strength compared to the actual value.

Table 7. ANOVA for yield strength model

Source	Sum of Squares	df	Mean Square	F-value	p-value		% Contribution
Model	12964.25	16	810.27	27.45	< 0.0001	significant	
A-TS	538.97	1	538.97	18.26	0.0021	significant	5.92
B-RS	2354.34	1	2354.34	79.76	< 0.0001	significant	25.87
C-TA	620.70	1	620.70	21.03	0.0013	significant	6.82
D-SD	780.49	1	780.49	26.44	0.0006	significant	8.58
E-TPP	1636.23	3	545.41	18.48	0.0003	significant	5.99
AB	170.67	1	170.67	5.78	0.0396	significant	1.87
AC	44.59	1	44.59	1.51	0.2502		0.49
AD	518.45	1	518.45	17.56	0.0023	significant	5.70
BC	835.24	1	835.24	28.30	0.0005	significant	9.18
BD	346.75	1	346.75	11.75	0.0075	significant	3.81
DE	729.47	3	243.16	8.24	0.0060	significant	2.67
A^2	1283.45	1	1283.45	43.48	< 0.0001	significant	14.10
Residual	265.64	9	29.52				
Lack of Fit	50.75	4	12.69	0.2952	0.8697	not significant	
Pure Error	214.90	5	42.98				
Cor Total	13229.90	25					

Table 8. Fit statistics for yield strength model

Standard deviation	5.43	**R^2**	0.9799
Mean	226.48	**Adjusted R^2**	0.9442
C.V. %	2.40	**Predicted R^2**	0.8092
		Adequate Precision	25.0802

C. Effect of Process Parameters on Percentage Elongation

For percentage elongation, interaction effects of tilt angle-shoulder diameter (CD) and rotational speed-tilt angle (BC) were identified as significant based on the ANOVA results shown in the Table 9. The maximum predicted value for percentage elongation of 4.74844% at desirability of 1 was obtained at rotational speed of 900 rpm, shoulder diameter of 16 mm and tilt angle of 0.5^0. At a rotational speed of 900 rpm, the percentage elongation was constant with respect to tilt angle. At a tilt angle of 0.5^0, the percentage elongation was gradually decreasing with respect to the rotational speed. At a shoulder diameter of 16 mm, the percentage elongation was constant with respect to the tilt angle. At a tilt angle of 0.5^0, the percentage elongation decreased with respect to shoulder diameter. The colour coding in the contour plots in the Figure 6 and Figure 7 suggest that range of process parameters selected were good enough to get high value of percentage elongation.

a) Models Developed for percentage elongation: The mathematical models for tensile elongation in terms of process parameters were developed by the RSM for the four tool pin profiles. The regression models, which are reduced quadratic models, can predict the elongation for the process parameters values within the selected range. The substitution of process parameters in the regression model should be with their original units. The models for elongation for different tool pin profiles are shown in the Eq. (10) – Eq. (13).

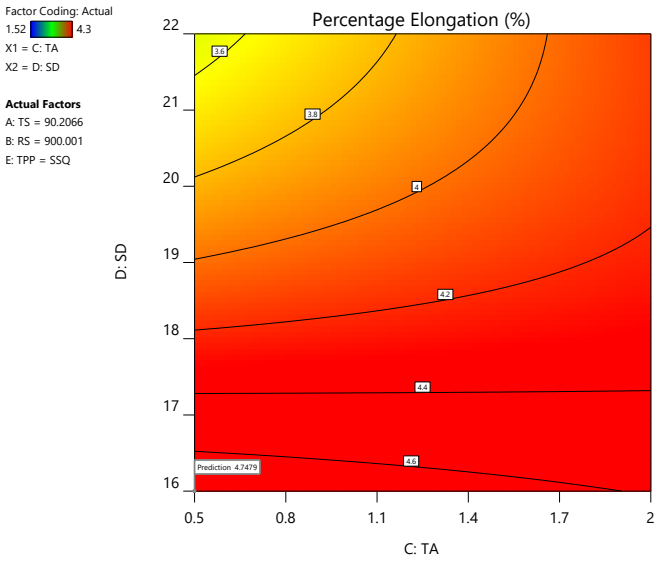

Fig. 7 Effects of TA and SD on percentage elongation

TPP: **SCL**

ELONATION = +27.88405 -0.105499*TS -0.003951*RS -3.77473*TA -1.47352*SD -0.002639*TS*TA +0.006098*TS*SD +0.001396*RS*TA +0.000136*RS*SD +0.084652*TA*SD -4.64961E-07*RS² +0.014633*SD² (10)

TPP: **TCL**

ELONATION = +26.25632 -0.105499*TS -0.003951*RS -3.20767*TA -1.47352*SD -0.002639*TS*TA +0.006098*TS*SD +0.001396*RS*TA +0.000136*RS*SD +0.084652*TA*SD -4.64961E-07*RS² +0.014633*SD² (11)

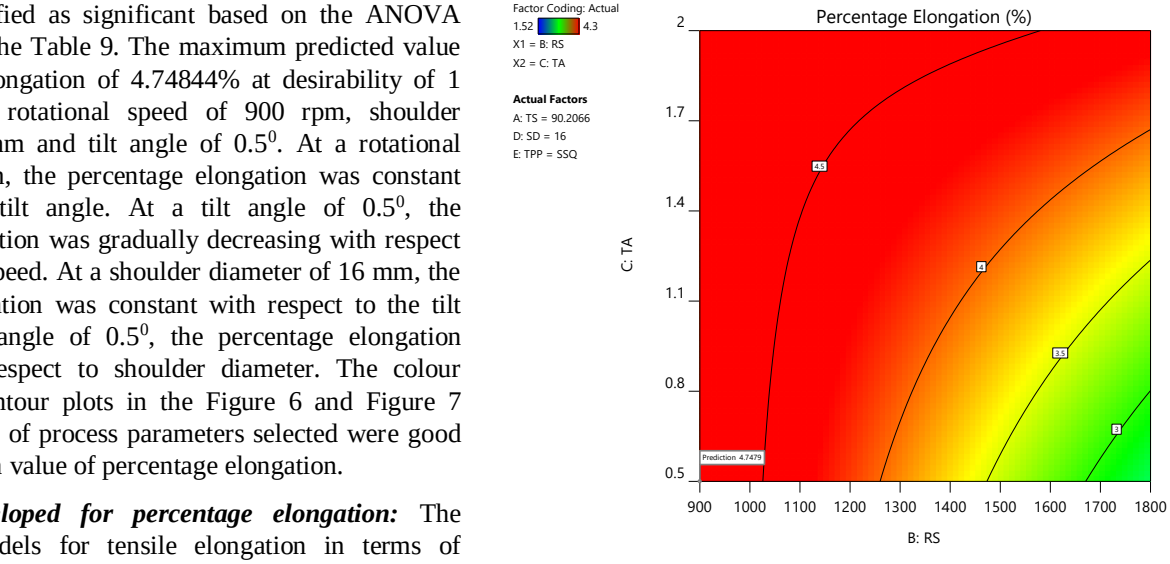

Fig. 6 Effects of RS and TA on percentage elongation

TPP: **SSQ**

ELONATION = +27.31738 -0.105499*TS -0.003951*RS -2.47795*TA -1.47352*SD -0.002639*TS*TA +0.006098*TS*SD +0.001396*RS*TA +0.000136*RS*SD +0.084652*TA*SD -4.64961E-07*RS² +0.014633*SD² (12)

TPP: **TSQ**

ELONATION = +25.56927 -0.105499*TS -0.003951*RS -2.61169*TA -1.47352*SD -0.002639*TS*TA +0.006098*TS*SD +0.001396*RS*TA +0.000136*RS*SD +0.084652*TA*SD -4.64961E-07*RS² +0.014633*SD² (13)

b) Adequacy of the Models: The mathematical models developed in the section 4.3.1 were validated by the analysis of variance (ANOVA) and the results are shown in the Table 9. The models developed for elongation were adequate and significant as its F-value is large (236.21) and p-value is very small (<0.0001). The lack of fit of the models were not significant as its F-value is very small (2.09) and p-value is greater than 0.05 (0.2198). All the process parameters except tilt angle along with the interactive terms AD, BC, BD, CD, CE, B^2 and D^2 were significant terms in the model as their respective p-values are less than 0.05.

The fit statistics of the models developed for the elongation are shown in the Table 10. The high value of coefficient of determination R^2 (0.998) indicates the adequacy and fitness of the model. The difference between adjusted R^2 (0.9938) and predicted R^2 (0.9537) is less than 0.2, which is a good indicator of fitness of the model. A

minimum value of 4 for the adequate precision indicates the adequate signal, which is 59.1349 in this case. Very small value of standard deviation (0.0577) compared to the mean (2.59) indicates the accuracy of the model to predict the elongation compared to the actual value.

Table 9. ANOVA for tensile elongation model

Source	Sum of Squares	df	Mean Square	F-value	p-value		% Contribution
Model	13.36	17	0.7860	236.21	< 0.0001	significant	
A-TS	0.0702	1	0.0702	21.09	0.0018	significant	0.99
B-RS	1.15	1	1.15	345.66	< 0.0001	significant	16.29
C-TA	0.0023	1	0.0023	0.6845	0.4320		0.03
D-SD	1.34	1	1.34	403.70	< 0.0001	significant	19.02
E-TPP	5.31	3	1.77	532.17	< 0.0001	significant	25.08
AC	0.0118	1	0.0118	3.55	0.0963		0.17
AD	0.8765	1	0.8765	263.42	< 0.0001	significant	12.41
BC	0.5465	1	0.5465	164.23	< 0.0001	significant	7.74
BD	0.0939	1	0.0939	28.21	0.0007	significant	1.33
CD	0.0711	1	0.0711	21.37	0.0017	significant	1.01
CE	0.7607	3	0.2536	76.21	< 0.0001	significant	3.59
B^2	0.0232	1	0.0232	6.97	0.0297	significant	0.33
D^2	0.0550	1	0.0550	16.52	0.0036	significant	0.78
Residual	0.0266	8	0.0033				
Lack of Fit	0.0148	3	0.0049	2.09	0.2198	not significant	
Pure Error	0.0118	5	0.0024				
Cor Total	13.39	25					

Table 10. Fit statistics for tensile elongation model

Standard deviation	0.0577	**R^2**	0.9980
Mean	2.59	**Adjusted R^2**	0.9938
C.V. %	2.23	**Predicted R^2**	0.9537
		Adequate Precision	59.1349

D. Effect of Process Parameters on Hardness of Weld Zone

For hardness of weld zone, interaction effects of transverse speed-tilt angle (AC) and rotational speed-tilt angle (BC) were identified as significant terms based on the ANOVA results shown in the Table 11. The maximum predicted value for hardness of weld zone of 108.536 at desirability of 1 was obtained at traverse speed of 90 mm/min, rotational speed of 900 rpm and tilt angle of 0.5^0. At a traverse speed of 90 mm/min the hardness of weld zone was decreasing slightly with respect to tilt angle. At a tilt angle of 0.5^0 the hardness of weld zone reached peak value at a traverse speed of 90 mm/min, and then decreased drastically. At a tilt angle of 0.5^0, the hardness of weld zone was constant with respect to rotational speed. At a rotational speed of 900 rpm, the hardness of weld zone decreased slightly with respect to tilt angle 0.5^0. The colour coding in the contour plots in the Figure 8 and Figure 9 suggest that better values for hardness of weld zone will be resulted at the lower values than the lower limits of rotational speed and tilt angle taken in this work.

a) Models Developed for Hardness of Weld Zone: The mathematical models for hardness of weld zone in terms of process parameters were developed by the RSM for the four tool pin profiles. The regression models, which are reduced quadratic models, can predict the hardness of weld zone for the process parameters values within the selected range. The substitution of process parameters in the regression model should be with their original units. The models for hardness of weld zone for different tool pin profiles are shown in the Eq. (14) – Eq. (17).

TPP: **SCL**

Hardness of Weld Zone= +128.59693 -0.133680*TS +0.007792*RS -33.89699*TA -0.533087*SD +0.249634*TS*TA +0.001486*RS*TA -0.000726*TS² +1.85920*TA² (14)

TPP: **TCL**

Hardness of Weld Zone= +124.56014 -0.077861*TS +0.010019*RS -33.89699*TA -0.533087*SD +0.249634*TS*TA +0.001486*RS*TA -0.000726*TS² +1.85920*TA² (15)

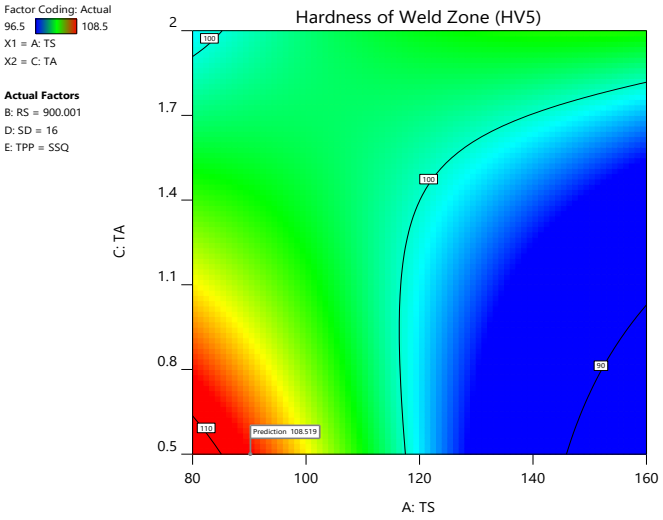

Fig. 8 Effects of TS and TA on hardness of weld zone

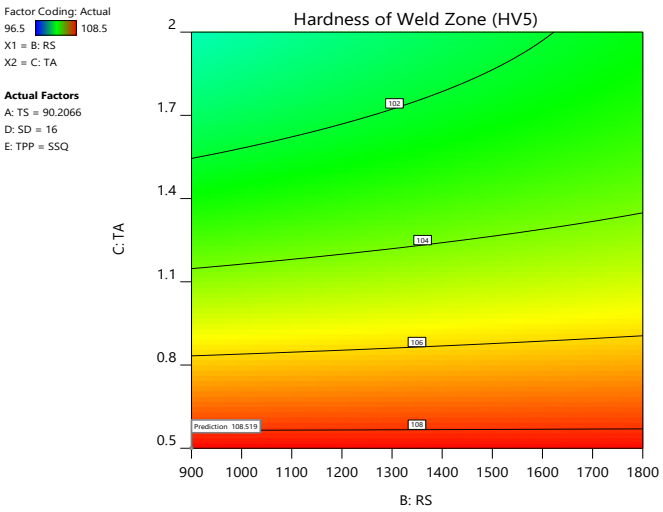

Fig. 9 Effects of RS and TA on hardness of weld zone

TPP: **SSQ**

Hardness of Weld Zone= +154.02155 -0.285921*TS -0.000797*RS -33.89699*TA -0.533087*SD +0.249634*TS*TA +0.001486*RS*TA -0.000726*TS² +1.85920*TA² (16)

TPP: **TSQ**

Hardness of Weld Zone= +140.36042 -0.195234*TS +0.006486*RS -33.89699*TA -0.533087*SD +0.249634*TS*TA +0.001486*RS*TA -0.000726*TS² +1.85920*TA² (17)

b) Adequacy of the Models: The mathematical models developed in the section 4.4.1 were validated by the analysis of variance (ANOVA) and the results are shown in the Table 11. The models developed for hardness of weld zone were adequate and significant as its F-value is large (50.62) and p-value is very small (<0.0001). The lack of fit of the models were not significant as its F-value is very small (0.0972) and p-value is greater than 0.05 (0.9582). The terms B (RS), D (SD), E (TPP), AC, AE, BE and A^2 were significant terms in the model as their respective p-values are less than 0.05.

The fit statistics of the models developed for the hardness of weld zone are shown in the Table 12. The high value of coefficient of determination R^2 (0.9908) indicates the adequacy and fitness of the model. The difference between adjusted R^2 (0.9712) and predicted R^2 (0.9411) is less than 0.2, which is a good indicator of fitness of the model. A minimum value of 4 for the adequate precision indicates the adequate signal, which is 28.6998 in this case. Very small value of standard deviation (0.5063) compared to mean (104.58) indicates the accuracy of the model to predict the hardness of the weld zone compared to the actual value.

Table 11. ANOVA for hardness of weld zone model

Source	Sum of Squares	df	Mean Square	F-value	p-value		% Contribution
Model	220.55	17	12.97	50.62	< 0.0001	significant	
A-TS	0.9370	1	0.9370	3.66	0.0922		0.39

B-RS	89.82	1	89.82	350.43	< 0.0001	significant	37.15
C-TA	0.0021	1	0.0021	0.0080	0.9308		0.00
D-SD	13.38	1	13.38	52.19	< 0.0001	significant	5.53
E-TPP	102.55	3	34.18	133.36	< 0.0001	significant	14.14
AC	71.28	1	71.28	278.11	< 0.0001	significant	29.48
AE	28.60	3	9.53	37.19	< 0.0001	significant	3.94
BC	0.6328	1	0.6328	2.47	0.1548		0.26
BE	16.71	3	5.57	21.73	0.0003	significant	2.30
A^2	2.76	1	2.76	10.78	0.0111	significant	1.14
C^2	0.6678	1	0.6678	2.61	0.1452		0.28
Residual	2.05	8	0.2563				
Lack of Fit	0.1130	3	0.0377	0.0972	0.9582	not significant	
Pure Error	1.94	5	0.3875				
Cor Total	222.60	25					

Table 12. Fit statistics for hardness of weld zone model

Standard deviation	0.5063	**R^2**	0.9908
Mean	104.58	**Adjusted R^2**	0.9712
C.V. %	0.4841	**Predicted R^2**	0.9411
		Adequate Precision	28.6998

E. Effect of Process Parameters on Hardness of Heat Affected Zone

For hardness of heat affected zone, interaction effects of transverse speed-rotational speed (AB) and rotational speed-tilt angle (BC) were identified as significant based on the ANOVA results shown in the Table 13. The maximum predicted value for hardness of weld zone of 121.612 at desirability of 1 was obtained at traverse speed of 90 mm/min, rotational speed of 900 rpm and tilt angle of 0.5^0. At a traverse speed of 90 mm/min the hardness of heat affected zone was decreasing slightly with respect to rotational speed. At a rotational speed of 900 rpm, the hardness of heat affected zone was constant with respect to traverse speed. At a tilt angle of 0.5^0, hardness of heat affected zone was decreasing slightly with respect to rotational speed. At a rotational speed of 900 rpm, hardness of heat affected zone was decreasing with respect to the tilt

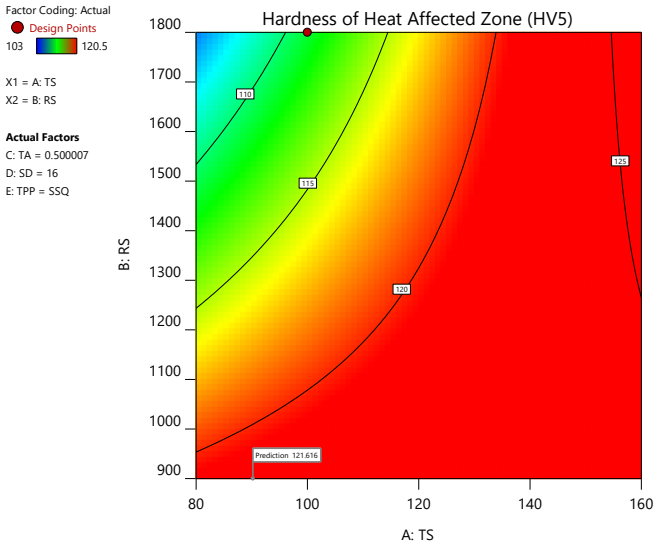

Fig. 10 Effects of RS and TS on hardness of heat affected zone

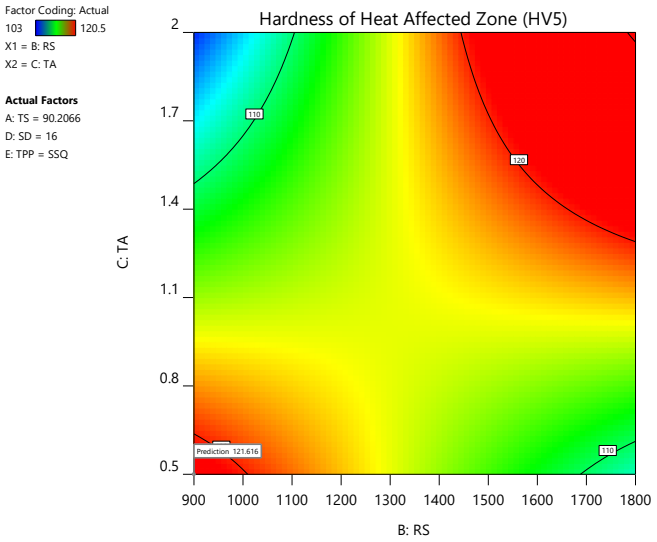

Fig. 11 Effects of RS and TA on hardness of heat affected zone

angle. The colour coding in the contour plots in the Figure 10 and Figure 11 suggest that the range of values selected for traverse speed, rotational speed and tilt angle were good enough to get high value of hardness of heat affected zone.

a) Models Developed for Hardness of Heat Affected Zone: The mathematical models for hardness of heat affected zone in terms of process parameters were developed by the RSM for the four tool pin profiles. The regression models, which are reduced quadratic models, can predict the hardness of heat affected zone for the process parameters values within the selected range. The substitution of process parameters in the regression model should be with their original units. The models for hardness of heat affected zone for different tool pin profiles are shown in the Eq. (18) – Eq. (21).

TPP: **SCL**

Hardness of HAZ= +307.72758 -0.085174*TS - 0.069629*RS -51.06421*TA -11.82203*SD +0.000245*TS*RS +0.029476*RS*TA +0.797757*TA*SD - 0.000394*TS² +0.252623*SD² (18)

TPP: **TCL**

Hardness of HAZ= +295.45717 -0.085174*TS - 0.070268*RS -51.06421*TA -11.03519*SD +0.000245*TS*RS +0.029476*RS*TA +0.797757*TA*SD - 0.000394*TS² +0.252623*SD² (19)

TPP: **SSQ**

Hardness of HAZ= +245.94232 -0.085174*TS - 0.051550*RS -51.06421*TA -9.10528*SD +0.000245*TS*RS +0.029476*RS*TA +0.797757*TA*SD - 0.000394*TS² +0.252623*SD² (20)

TPP: **TSQ**

Hardness of HAZ= +272.10786 -0.085174*TS - 0.077058*RS -51.06421*TA -9.19776*SD +0.000245*TS*RS +0.029476*RS*TA +0.797757*TA*SD - 0.000394*TS² +0.252623*SD² (21)

b) Adequacy of the Models: The mathematical models developed in the section 4.5.1 were validated by the analysis of variance (ANOVA) and the results are shown in the Table 13. The models developed for hardness of heat affected zone were adequate and significant as its F-value is large (14.64) and p-value is very small (0.0007). The lack of fit of the models were not significant as its F-value is very small (0.0263) and p-value is greater than 0.05 (0.9742). The terms A (TS), B (RS), E (TPP), AB, BC, BE and DE were significant terms in the model as their respective p-values are less than 0.05.

The fit statistics of the models developed for the hardness of heat affected zone are shown in the Table 14. The high value of coefficient of determination R^2 (0.9741) indicates the adequacy and fitness of the model. The difference between adjusted R^2 (0.9076) and predicted R^2 (0.8153) is less than 0.2, which is a good indicator of fitness of the model. A minimum value of 4 for the adequate precision indicates the adequate signal, which is 15.2147 in this case. The small value of standard deviation (1.37) compared to mean (112.34) indicates the accuracy of the model to predict the hardness of heat affected zone compared to the actual value.

Table 13. ANOVA for hardness of heat affected zone model

Source	Sum of Squares	df	Mean Square	F-value	p-value		% Contribution
Model	492.26	18	27.35	14.64	0.0007	significant	
A-TS	57.94	1	57.94	31.01	0.0008	significant	17.56
B-RS	29.94	1	29.94	16.03	0.0052	significant	9.08
C-TA	5.45	1	5.45	2.92	0.1313		1.65
D-SD	0.1887	1	0.1887	0.1010	0.7599		0.06
E-TPP	300.57	3	100.19	53.62	< 0.0001	significant	30.36
AB	11.08	1	11.08	5.93	0.0451	significant	3.36
BC	69.34	1	69.34	37.11	0.0005	significant	21.01

BE	35.27	3	11.76	6.29	0.0213	significant	3.56
CD	3.46	1	3.46	1.85	0.2156		1.05
DE	24.90	3	8.30	4.44	0.0477	significant	2.51
A^2	0.6034	1	0.6034	0.3230	0.5876		0.18
D^2	4.37	1	4.37	2.34	0.1699		1.32
Residual	13.08	7	1.87				
Lack of Fit	0.1359	2	0.0680	0.0263	0.9742	not significant	
Pure Error	12.94	5	2.59				
Cor Total	505.34	25					

Table 14. Fit statistics of hardness of heat affected zone model

Standard deviation	1.37	**R^2**	0.9741
Mean	112.34	**Adjusted R^2**	0.9076
C.V. %	1.22	**Predicted R^2**	0.8153
		Adequate Precision	15.2147

F. Effects of Process Parameters on Bending Load

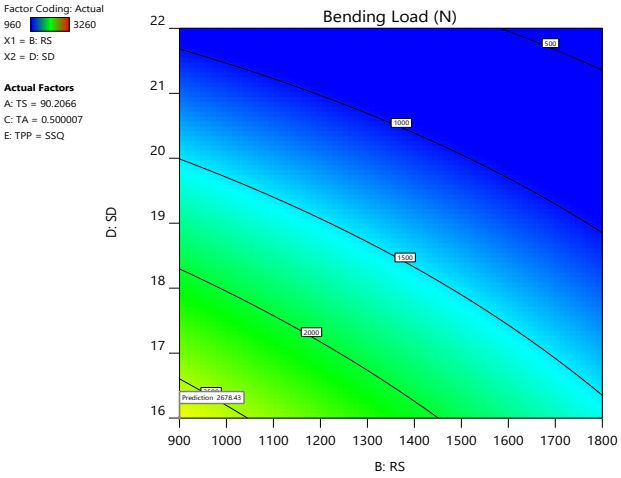

Fig. 12 Effects of RS and SD on bending load

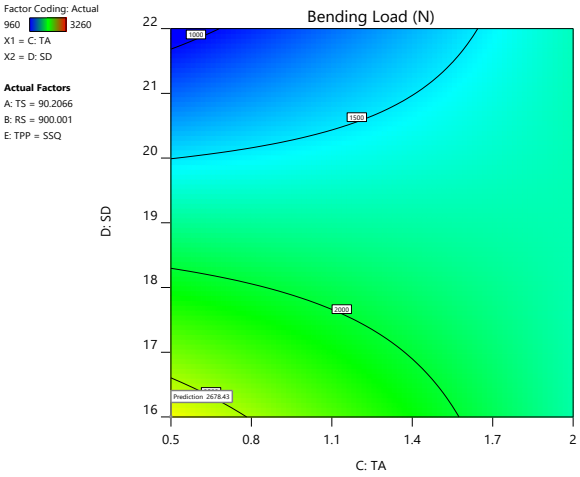

Fig. 13 Effects of SD and TA on bending load

For bending load, interaction effects of rotational speed-shoulder diameter (BD) and tilt angle-shoulder diameter (CD) were identified as significant terms based on the ANOVA results shown in the Table 15. The maximum predicted value for bending load of 2679.42N at a desirability of 0.747574 was obtained at rotational speed of 900 rpm, tilt angle of 0.5^0 and shoulder diameter of 16 mm. At a rotational speed of 900 rpm, the bending load was decreasing gradually with respect to shoulder diameter. At a shoulder diameter of 16 mm, the bending load was decreasing gradually with respect to rotational speed. At a tilt angle of 0.5^0, the bending load was decreasing gradually with respect to shoulder diameter. At a shoulder diameter of 16 mm, the bending load was constant with respect to tilt angle. The colour coding in the contour plots in the Figure 12 and Figure 13 suggest that better values for bending load will be resulted at the lower values than the lower limits of rotational speed, tilt angle and shoulder diameter taken in this work.

b) Models Developed for Bending Load: The mathematical models for bending load in terms of process parameters were developed by the RSM for the four tool pin profiles. The regression models, which are reduced quadratic models, can predict the bending load for the process parameters values within the selected range. The substitution of process parameters in the regression model should be with their original units. The models for bending load for different tool pin profiles are shown in the Eq. (22) – Eq. (25).

TPP: **SCL**

Bending Load= +15174.17365 -47.97324*TS -2.92960*RS -3698.55739*TA -489.20615*SD +0.106132*RS*SD +191.69698*TA*SD +0.170905*TS^2 (22)

TPP: **TCL**

Bending Load= +7909.06796 -47.97324*TS -2.92960*RS -3698.55739*TA -87.55704*SD +0.106132*RS*SD

+191.69698*TA*SD +0.170905*TS² (23)

TPP: **SSQ**

Bending Load= +14826.62431 -47.97324*TS -2.92960*RS -3698.55739*TA -486.70835*SD +0.106132*RS*SD +191.69698*TA*SD +0.170905*TS² (24)

TPP: **TSQ**

Bending Load= +16162.79300 -47.97324*TS -2.92960*RS -3698.55739*TA -483.56572*SD +0.106132*RS*SD +191.69698*TA*SD +0.170905*TS² (25)

c) Adequacy of the Models: The mathematical models developed in the section 4.6.1 were validated by the analysis of variance (ANOVA) and the results are shown in the Table 15. The models developed for bending load were adequate and significant as its F-value is large (26.56) and p-value is very small (<0.0001). The lack of fit of the models were not significant as its F-value is very small (0.8946) and p-value is greater than 0.05 (0.57). The terms A (TS), B (RS), E (TPP), CD and DE were significant terms in the model as their respective p-values are less than 0.05.

The fit statistics of the models developed for the bending load are shown in the Table 16. The high value of coefficient of determination R^2 (0.9664) indicates the adequacy and fitness of the model. The difference between adjusted R^2 (0.93) and predicted R^2 (0.8578) is less than 0.2, which is a good indicator of fitness of the model. A minimum value of 4 for the adequate precision indicates the adequate signal, which is 16.2858 in this case. The small value of standard deviation (5.43) compared to the mean (1754.23) indicates the accuracy of the model to predict the bending load compared to the actual value.

Table 15. ANOVA for bending load model

Source	Sum of Squares	df	Mean Square	F-value	p-value		% Contribution
Model	1.040E+07	13	7.997E+05	26.56	< 0.0001	significant	
A-TS	6.778E+05	1	6.778E+05	22.51	0.0005	significant	10.13
B-RS	1.837E+06	1	1.837E+06	61.02	< 0.0001	significant	27.47
C-TA	47691.99	1	47691.99	1.58	0.2321		0.71
D-SD	17681.13	1	17681.13	0.5873	0.4583		0.26
E-TPP	4.952E+06	3	1.651E+06	54.83	< 0.0001	significant	24.69
BD	57420.03	1	57420.03	1.91	0.1925		0.86
CD	7.994E+05	1	7.994E+05	26.55	0.0002	significant	11.95
DE	1.938E+06	3	6.462E+05	21.46	< 0.0001	significant	9.66
A^2	1.263E+05	1	1.263E+05	4.20	0.0630		1.89
Residual	3.613E+05	12	30106.77				
Lack of Fit	2.009E+05	7	28697.32	0.8946	0.5700	not significant	
Pure Error	1.604E+05	5	32080.00				
Cor Total	1.076E+07	25					

Table 16. Fit statistics for bending load model

Standard deviation	173.51	**R^2**	0.9664
Mean	1754.23	**Adjusted R^2**	0.9300
C.V. %	9.89	**Predicted R^2**	0.8578
		Adequate Precision	16.2858

G. Effect of Process Parameters on Width of Heat Affected Zone

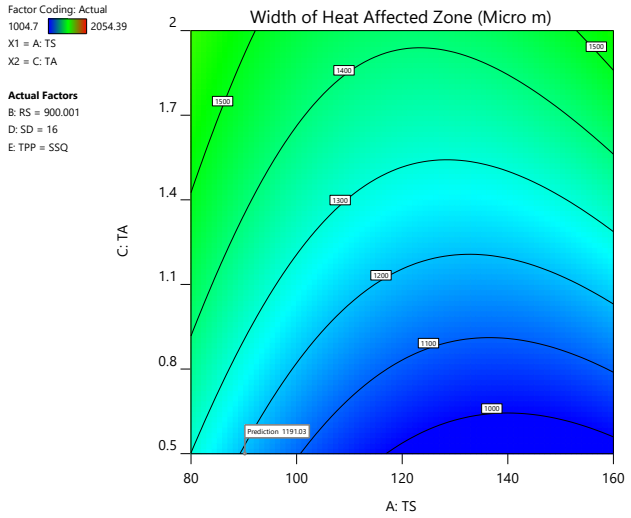

Fig. 14 Effects of TS and TA on width of heat affected zone

For width of heat affected zone, interaction effects of transverse speed-tilt angle (AC) and rotational speed-tilt angle (BC) were identified as significant terms based on the ANOVA results shown in the Table 17. The maximum predicted value for width of heat affected zone of 1191.59 µm at a desirability of 0.821952 was obtained at traverse speed of 90 mm/min, rotational spedd of 900 rpm and tilt

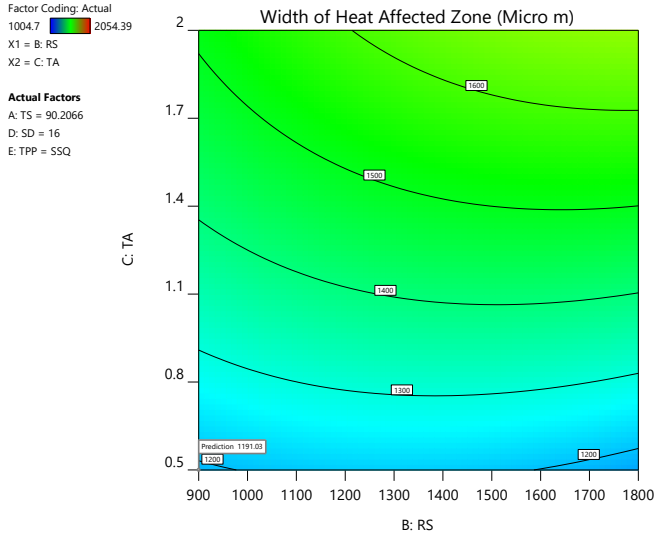

Fig. 15 Effects of RS and TA on width of heat affected zone

angle of 0.5^0. At a traverse speed of 90 mm/min, the width of heat affected zone was increasing gradually with respect to tilt angle. At a tilt angle of 0.5^0, the width of heat affected zone was decreasing up to a traverse speed of 90mm/min and thereafter remains constant with respect to traverse speed. At a tilt angle of 0.5^0, width of heat affected zone was increasing slightly with respect to rotational speed. At a rotational speed of 900 rpm, width of heat affected zone was increasing with respect to the tilt angle. The colour coding in the contour plots in the Figure 14 and Figure 15 suggest that the range of values selected for traverse speed, rotational speed and tilt angle were good enough to get low value of width of heat affected zone.

a) Models Developed for Width of Heat Affected Zone: The mathematical models for width of heat affected zone in terms of process parameters were developed by the RSM for the four tool pin profiles. The regression models, which are reduced quadratic models, can predict the width of heat affected zone for the process parameters values within the selected range. The substitution of process parameters in the regression model should be with their original units. The models for width of heat affected zone for different tool pin profiles are shown in the Eq. (26) – Eq. (29).

TPP: **SCL**

Width of HAZ= +7891.8562 -34.88706*TS +0.365835*RS -5.16371*TA -542.11627*SD +2.39388*TS*TA +0.13713*RS*TA +0.093453*TS² -0.000169*RS² -48.21493*TA² +16.3685*SD² (26)

TPP: **TCL**

Width of HAZ= +6474.09645 -22.79543*TS +0.365835*RS -5.16371*TA -542.11627*SD +2.39388*TS*TA +0.13713*RS*TA +0.093453*TS² -0.000169*RS² -48.21493*TA² +16.3685*SD² (27)

TPP: **SSQ**

Width of HAZ= +7065.87632 -27.70088*TS +0.365835*RS -5.16371*TA -542.11627*SD +2.39388*TS*TA +0.13713*RS*TA +0.093453*TS² -0.000169*RS² -48.21493*TA² +16.3685*SD² (28)

TPP: **TSQ**

Width of HAZ= +7691.05115 -32.96224*TS +0.365835*RS -5.16371*TA -542.11627*SD +2.39388*TS*TA +0.13713*RS*TA+0.093453*TS² -0.000169*RS² -48.21493*TA² +16.3685*SD² (29)

b) Adequacy of the models: The mathematical models developed in the section 4.7.1 were validated by the analysis of variance (ANOVA) and the results are shown in the Table 17. The models developed for bending load were adequate and significant as its F-value is large (111.83) and p-value is very small (<0.0001). The lack of fit of the models were not significant as its F-value is very small (0.4088) and p-value is greater than 0.05 (0.7966). The terms A (TS), C (TA), D (SD), E (TPP), AC, AE, BC, A^2 and D^2 were significant terms in the model as their respective p-values are less than 0.05.

The fit statistics of the models developed for the yield strength are shown in the Table 18. The high value of coefficient of determination R^2 (0.995) indicates the adequacy and fitness of the model. The difference between

adjusted R^2 (0.9861) and predicted R^2 (0.9509) is less than 0.2, which is a good indicator of fitness of the model. A minimum value of 4 for the adequate precision indicates the adequate signal, which is 38.06 in this case. The small value of standard deviation (32.81) compared to the mean (1568.16) indicates the accuracy of the model to predict the width of the heat affected zone compared to the actual value.

Table 17. ANOVA for width of heat affected zone model

Source	Sum of Squares	df	Mean Square	F-value	p-value		% Contribution
Model	1.926E+06	16	1.204E+05	111.83	< 0.0001	significant	
A-TS	68392.19	1	68392.19	63.52	< 0.0001	significant	4.68
B-RS	4580.74	1	4580.74	4.25	0.0692		0.31
C-TA	3.316E+05	1	3.316E+05	307.93	< 0.0001	significant	22.68
D-SD	7.451E+05	1	7.451E+05	692.04	< 0.0001	significant	50.96
E-TPP	30054.05	3	10018.02	9.30	0.0040	significant	0.68
AC	11523.94	1	11523.94	10.70	0.0097	significant	0.79
AE	1.512E+05	3	50399.50	46.81	< 0.0001	significant	3.45
BC	6270.40	1	6270.40	5.82	0.0390	significant	0.43
A^2	72654.69	1	72654.69	67.48	< 0.0001	significant	4.97
B^2	3097.17	1	3097.17	2.88	0.1241		0.21
C^2	2342.10	1	2342.10	2.18	0.1743		0.16
D^2	35313.39	1	35313.39	32.80	0.0003	significant	2.42
Residual	9690.29	9	1076.70				
Lack of Fit	2388.06	4	597.02	0.4088	0.7966	not significant	
Pure Error	7302.23	5	1460.45				
Cor Total	1.936E+06	25					

Table 18. Fit statistics for width of heat affected zone model

Standard deviation	32.81	**R^2**	0.9950
Mean	1568.16	**Adjusted R^2**	0.9861
C.V. %	2.09	**Predicted R^2**	0.9509
		Adequate Precision	38.0600

H. Optimization of Process Parameters

The multi-optimization problem was solved by the desirability approach in the response surface methodology (RSM). Though this desirability approach is primitive, it is simple, flexible and readily available in the RSM software. Software 'Design Expert 12' was used to find the desirability values of responses and the combined desirability value.

The desirability values of individual responses and combined desirability of all the responses were shown in the figure 16. The optimum process parameters obtained from this approach were: traverse speed-90 mm/min, rotational speed-900 rpm, tilt angle-0.5^0, shoulder diameter-16 mm and straight square (SSQ) tool pin profile. The predicted values of responses for the optimum process parameters were: tensile strength-337.36 MPa, yield strength-324.59 MPa, percentage elongation-4.75%, hardness of weld zone-108.52 (HV5), hardness of heat affected zone-121.62 (HV5), bending load-2678.43 N and width of heat affected zone-1191.034 µm. The combined desirability obtained from the analysis was 0.918053, which was fairly good.

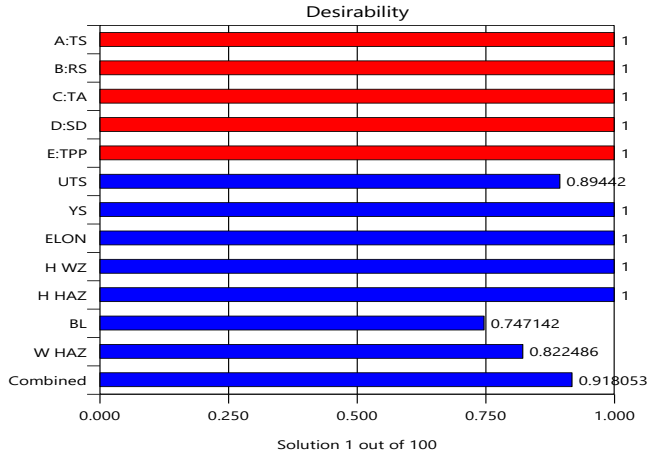

Fig. 16 Desirability values for parameters and responses

V. CONCLUSIONS

The friction stir welding was successfully carried according to the design of experiments for the selected values of process parameters. The following conclusions were drawn:

1. The predicted values of the responses by the regression models developed for the friction stir weld joints of AA2050-T84 aluminium alloy were in good agreement with the experimental values. The variation between predicted values and experimental values was within ±10% at 95% confidence level.
2. The rotational speed and tool pin profile were the significant process parameters for all the responses evaluated except for the width of the heat affected zone. For the width of the heat affected zone, shoulder diameter and tilt angle were the most significant process parameters.
3. The weld joints prepared using straight square tool profile with a transverse speed of 90 mm/min, rotational speed of 900 rpm, tilt angle of 0.5^0 and shoulder diameter of 16 mm resulted in superior joint.

In the present work process parameters and all the responses were given equal importance in optimization process. Varied importance for the responses may be decided for a particular application and the investigation may be carried accordingly. The optimum values of rotational speed, tilt angle and shoulder diameter were at the lower limits of the ranges selected. Hence further work may be carried by selecting lower values than the lower limits for the above process parameters.

REFERENCES

[1] Loureiro.A, Leitao.R.M, Rodrigues.D.M and Vilaca., Friction stir welding of automotive aluminium alloys, Welding in the world. 51 (2007) 433-440.

[2] R. Nandan, T. DebRoy and H.K.D.H. Bhadeshia, Recent advances in friction stir welding process, weldment structure and properties, Progress in Material Science. 53(6) (2008) 980-1023.

[3] CG Rhodes, MW Mahoney and WH Bingel, Effect of friction stir welding on microstructure of 7075 aluminium, Scripta Materialia. 36 (1997) 69-75.

[4] MW Mahoney, CG Rhodes, JG Flintoff, RA Spurling and WH Bingel, Properties of friction-stir-welded 7075-T651 aluminium, Metallurgical and Materials Transactions A. 29 (1998) 1955-1964.

[5] Stephan W.Kallee, E.Dave Nicholas and Wayne M.Thomas, Friction Stir Welding - Invention, Innovations and Applications, INALCO 2001, 8th International Conference on joints in Aluminium, Munich, Germany, 28-30 March 2001.

[6] ASM hand book, Volume 2B, Properties and Selection of Aluminium Alloys 2019.

[7] G.Elatharasan and V.S.Senthil Kumar, Optimization of friction stir welding parameters for dissimilar aluminium alloys using RSM, Procedia Engineering. 38 (2012) 3477-3481.

[8] A.Heidarzadeh, A.Mahoudi and E.Nazari, Tensile behavior of friction stir welding AA6061-T4 aluminum alloy joints, Materials and Design. 37 (2012) 166-173.

[9] R.Palanivel and P.Koshy Mathews, Prediction and optimization of process parameter of friction stir welded AA5083-H111 aluminum alloy using response surface methodology, Journal of Central South University. 19 (2012) 1-8.

[10] G.Elatharasan and V.S.Senthil Kumar, An experimental analysis and optimization of process parameter on friction stir welding of AA6061-T6 aluminum alloy using RSM, Procedia Engineering. 64 (2013) 1227-1234.

[11] Divya Deep Dhancholia, Anuj Sharma and Charit Vyas, Optimisation of Friction Stir Welding Parameters for AA6061 and AA7039 Aluminium Alloys by Response Surface Methodology (RSM), International Journal of Advanced Mechanical Engineering. 4(5) (2014) 565-571.

[12] Ramanjaneyulu Kadaganchi, Madhusudhan Reddy Gankidi and Hina Gokhale, Optimization of process parameters of aluminium alloy AA2014-T6 friction stir welds by response surface methodology, Defence Technology. 11 (2015) 209-219.

[13] A.Farzadi, M.Bahmani and D.F.Haghshenas, Optimization of Operating Parameters in Friction Stir Welding of AA7075-T6 Aluminum Alloy Using Response Surface Method, Arabian Journal for Science and Engineering. 42 (2017) 4905-4916.

[14] B.Ravi Sankar and P.Umamaheswarrao, Modelling and Optimisation of Friction Stir Welding on AA6061 Alloy, Materials today: Proceedings. 4(8) (2017) 7448-7456.

[15] A.Goyal and R.K.Garg, Modelling and optimization of friction stir welding parameters in joining 5086- H32 aluminium alloy, Scientia Iranica Transactions B: Mechanical Engineering. 26(4) (2019) 2407-2417.

[16] Boz Mustafa and Kurt Adem, The influence of stirrer geometry on bonding and mechanical properties in friction stirs welding process, Materials & Design. 25 (2004) 343–347.

[17] Cavaliere P, Campanile G, Panella F and Squillace A, Effect of Welding Parameters on Mechanical and Microstructural Properties of AA6056 Joints Produced by Friction Stir Welding, Journal of Material Processing Technology. 180 (2006) 263–270.

[18] Elangovan.K and Balasubramanian.V, Influences of pin profile and rotational speed of the tool on the formation of friction stir processing zone in AA2219 aluminium alloy, Materials Science and Engineering: A. 459 (2007) 7–18.

[19] Elangovan.K and Balasubramanian.V, Influences of tool pin profile and welding speed on the formation of friction stir processing zone in AA2219 aluminium alloy, Journal of materials processing technology. 200 (2008) 163–175.

[20] Lombard H, Hattingh DG, Steuwer A and James MN, Effect of process parameters on the residual stresses in AA5083-H321 friction stir welds, Materials Science and Engineering: A. 501 (2009) 119–124.

[21] Kanwer S Arora, Sunil Pandey, Michael Sehaper and Rajneesh Kumar, Effect of process parameters on friction stir welding of aluminum alloy 2219-T87, International Journal of Advanced Manufacturing Technology. 50 (2010) 941-952.

[22] L.Karthikeyan and V.S.Senthil Kumar, Relationship between Process Parameters and Mechanical Properties of Friction Stir Processed AA6063-T6 Aluminum Alloy, Materials and Design. 32 (2011) 3085-3091.

[23] Z. Barlas and U. Ozsarac, Effects of FSW Parameters on Joint Properties of AlMg3 Alloy, Welding Journal. 91 (2012) 16s-22s.

[24] Muhsin.J.J, Moneer.H.Tolephih and Muhammed.A.M, Effect of Friction Stir Welding Parameters (Rotation and Traverse) speed on the Transient Temperature Distribution in Friction Stir Welding of AA 7020-T53, ARPN Journal of Engineering and Applied Sciences, 6(2) (2012) 61-66.

[25] K.Ramanjeneyulu, G.Madhusudhan Reddy, A.Venugopal Rao and R.Markandeya, Structure-Property Correlation of AA2014 Friction Stir Welds: Role of Tool Pin Profile, Journal of Materials Engineering and Performance. 22 (2013) 2224-2240.

[26] Suyash Tiwari, H.Chelladurai and Ashish Kumar Shukla, Parametric Analysis of Friction Stir Welding, 5th International & 26th All India Manufacturing Technology, Design and Research Conference, December 12th-14th, 2014, IIT Guwati, Assam, India.

[27] Ravindra S.Thube and Surjya K.Pal, Influence of tool pin profile and welding parameters on Friction stir weld formation and joint efficiency of AA5083 Joints produced by Friction Stir Welding, International Journal of Innovative Research in Advanced Engineering. 1(4) (2014) 1-8.

[28] Emad Salari, Mohammad Jahazi, Alireza Khodabandeh and Hadi Ghasemi-Nanesa, Influence of tool geometry and rotational speed on mechanical properties and defect formation in friction stir lap welded 5456 aluminum alloy sheets, Materials and Design. 58 (2014) 381-389.

[29] Joon-Tae Yoo, Jong-Hoon Yoon, Kyung-Ju Min and Ho-Sung Lee, Effect of Friction Stir Welding Process Parameters on Mechanical Properties and Macro Structure of Al-Li Alloy, Procedia Manufacturing. 2 (2015) 325-330.

[30] V.K.Parikh, A.D.Badgujar and N.D.Ghetiya, Multi-objective optimization of FSW process parameters using MOORA method, International Journal of Advances in Production and Mechanical Engineering. 3(2) (2017) 19-24.

[31] Shubham Verma, Meenu Gupta and Joy Prakash Misra, Performance evaluation of friction stir welding using machine learning approaches, MethodX. 5 (2018) 1048-1058.

[32] Shanavas Shamsudeen and John Edwin Raja Dhas, Optimization of Multiple Performance Characteristics of Friction Stir Welded joint with Grey Relational Analysis, Materials Research. 21(6) (2018) 1-14.

[33] Abuajila Raweni, Vidosav Majstorovic, Aleksandav Sedmak, Srdjan Tadic and Snezana Kirin, Optimization of AA5083 Friction Stir Welding Parameters Using Taguchi Method, Technical Gazette. 25(3) (2018) 861-866.

[34] M.Gomathisankar, M.Gangatharan and P.Pitchipoo, A Novel Optimization of Friction Stir Welding process Parameters on Aluminum Alloy 6061-T6, Materials today: PROCEEDINGS. 5(6) (2018) 14397-14404.

[35] P.Pradeep Kumar, Sk Ahmmad Basha and S.Sai Kumar, Optimization of Friction Stir Welding process parameters of Aluminium alloy AA7075-T6 by using Taguchi method, International Journal of Innovative Technology and Exploring Engineering. 8(12) (2019) 290-297.